


 Cite this: *RSC Adv.*, 2022, **12**, 23626

Synthesis of novel benzothiazole derivatives and investigation of their enzyme inhibitory effects against Alzheimer's disease†

Şevval Karaca,^{ab} Derya Osmaniye,^{ID, bc} Begüm Nurpelin Sağlık,^{ID, bc} Serkan Levent,^{bc} Sinem İlgin,^{ID, d} Yusuf Özkar,^{ID, *bc} Ahmet Çağrı Karaburun,^b Zafer Asım Kaplancıklı^{ID, b} and Nalan Gundogdu-Karaburun^b

The use of dual acetylcholinesterase (AChE)–monoamine oxidase B (MAO-B) inhibitors is a new approach in the treatment of Alzheimer disease (AD). In this work, 14 new benzothiazoles (**4a–4n**) were designed and synthesized. In biological activity studies, the AChE, butyrylcholinesterase (BChE), MAO-A and MAO-B inhibitory potentials of all compounds were evaluated using the *in vitro* fluorometric method. Additionally, amyloid beta (A β)-aggregation inhibitory effects of active compounds were evaluated by means of an *in vitro* kit-based method. The biological evaluation showed that compounds **4a**, **4d**, **4f**, **4h**, **4k** and **4m** displayed significant activity against AChE and MAO-B enzymes. Compound **4f** displayed inhibitory activity against AChE and MAO-B enzyme with IC₅₀ values of 23.4 ± 1.1 nM and 40.3 ± 1.7 nM, respectively. It has been revealed that compound **4f** may have the potential to inhibit AChE and MAO-B enzymes, as well as the ability to prevent the formation of beta amyloid plaques accumulated in the brains of patients suffering from AD. *In silico* studies also support the obtained biological activity findings. Compound **4f** provided strong interactions with the active site of both enzymes. In particular, the interaction of compound **4f** with flavin adenine dinucleotide (FAD) in the MAO-B enzyme active site is a promising and exciting finding.

 Received 20th June 2022
 Accepted 22nd July 2022

 DOI: 10.1039/d2ra03803j
rsc.li/rsc-advances

1. Introduction

Alzheimer's disease (AD), a devastating neurodegenerative disease, causes deficits in memory, thought, and behavior.¹ Many hypotheses have been proposed for the treatment of AD, including inhibition of cholinesterase, inhibition of amyloid protein (A β) formation, and inhibition of tau protein accumulation.² Cholinergic signaling is known to play a critical role in cognitive performance and cholinergic signaling has been observed to gradually disappear in AD. For this purpose, a treatment line has been established to treat symptoms using cholinesterase inhibitors.³ Several FDA-approved anti-AD drugs currently available clinically (such as cholinesterase inhibitors: donepezil, rivastigmine, galantamine) provide only partial relief of symptoms and cannot stop or reverse disease progression.⁴

^aDepartment of Biochemistry, Faculty of Pharmacy, Anadolu University, 26470 Eskişehir, Turkey

^bDepartment of Pharmaceutical Chemistry, Faculty of Pharmacy, Anadolu University, 26470 Eskişehir, Turkey. E-mail: yozkay@anadolu.edu.tr

^cCentral Analysis Laboratory, Faculty of Pharmacy, Anadolu University, 26470 Eskişehir, Turkey

^dDepartment of Pharmaceutical Toxicology, Faculty of Pharmacy, Anadolu University, 26470 Eskişehir, Turkey

† Electronic supplementary information (ESI) available. See <https://doi.org/10.1039/d2ra03803j>

Donepezil works in Alzheimer's disease specifically as an acetylcholinesterase (AChE) inhibitor at mild to moderate levels. However, donepezil has side effects such as nausea, diarrhea, weakness, dizziness, urinary incontinence, and insomnia. Donepezil may also cause gastrointestinal and neurological adverse reactions such as speech difficulties, involuntary tremors, and vomiting.^{5–9} Therefore, there is a need to develop new molecules in this field.

The enzymatic cavity of AChE is characterized by a nearly 20 Å deep narrow gorge, which is composed of two binding sites: the catalytic active site (CAS) at the bottom and the peripheral anionic site (PAS) near the entrance of the gorge.¹⁰

Plaques, or more likely their soluble oligomers, of A β peptides, whose aggregation and accumulation in the brain play a key role in the initiation and progression of AD, are neurotoxic. The discovery of the ability of PAS of AChE to induce β -amyloid aggregation has triggered an intense search for compounds that exhibit dual activity as inhibitors of AChE activity and A β aggregation.¹¹

It has been proven that the level of monoamine oxidase-B (MAO-B) is increased in Alzheimer's plaques and blood platelets of AD and Parkinson (PD) patients. This increase in MAO-B is most likely due to the following; it is due to the transcriptional upregulation of MAO-B in the protein and its



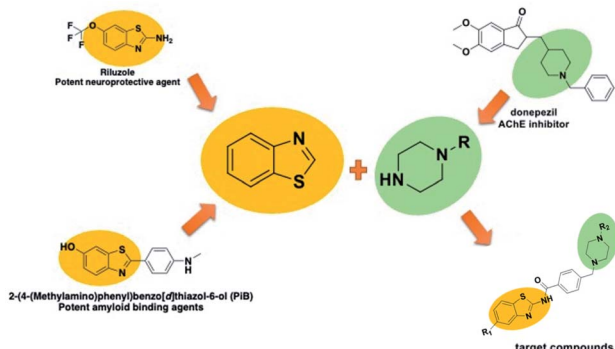


Fig. 1 Design of target compounds (4a–4n).

predominance in plaque-associated astrocytes in pathologically confirmed AD brains.¹²

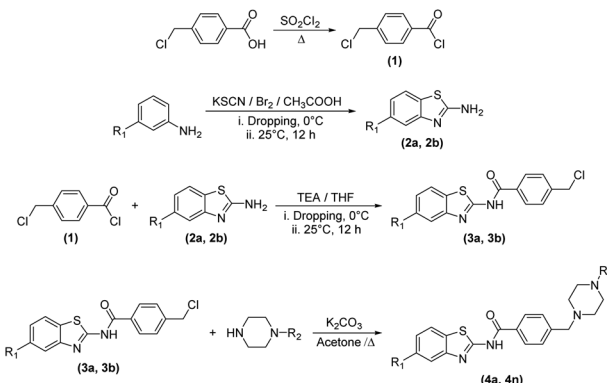
Compounds that co-inhibit the three formations mentioned above (AChE, A β plaque, MAO-B) will contribute significantly to this field. Recently, multifactorial agents have come to the fore. Because considering the age of the patient group, the use of a single agent that inhibits all of them instead of separate agents will also facilitate. It has been reported that benzothiazole ring provides all three of these effects.^{13–15} Thus, it was chosen as a pharmacophore in the main structure of our compounds.

In addition to the above-mentioned properties of the benzothiazole ring, it also has use as a neuroprotective and amyloid-inhibiting agent.^{16,17} In addition, it is known that the secondary amine derivatives (piperazine or piperidine in the structure of donepezil) is necessary for interaction with the CAS region of the enzyme.³ Also, the presence of these groups in the chemical structure provide the flexibility and thus contribute to binding properly to the gorge of the enzyme active site. Within the scope of this study, the compounds were designed to be similar in length to donepezil and to localize to the enzyme active site. In the light of this information, both benzothiazole and piperazine (as a secondary amine derivatives) were used in the structure of the target compounds (Fig. 1).

2. Result and discussion

2.1. Chemistry

In the scope of the present study, it was aimed to synthesize new compounds containing benzothiazole and piperazine groups in the same chemical structure. For this purpose, 14 new compounds were synthesized. Target compounds were obtained using a four-step reaction method. The synthesis pathway of the compounds is presented in Scheme 1. Initially, 4-(chloromethyl) benzoyl chloride (**1**) was synthesized using thionyl chloride. Secondly, 2-aminobenzothiazoles (**2a–2b**) derivatives were synthesized by means of ring closure reaction using bromine solution. Thirdly, 4-(chloromethyl)-N-(5,6-disubstituted benzothiazol-2-yl) benzamides (**3a–3b**) were obtained by means of reaction between 4-(chloromethyl) benzoyl chloride (**1**) and 2-aminobenzothiazoles (**2a–2b**). In the last step,



Comp.	R ₁	R ₂
2a	-H	-
2b	-OCH ₃	-
3a	-H	-
3b	-OCH ₃	-
4a	-H	-CH ₃
4b	-H	-CH ₂ CH ₃
4c	-H	-CH ₂ CH=CH ₂
4d	-H	-CH ₂ C≡CH
4e	-H	-CH(CH ₃) ₂
4f	-H	-CH ₂ CH ₂ N(CH ₃) ₂
4g	-H	-CH ₂ CH ₂ CH ₂ N(CH ₃) ₂
4h	-OCH ₃	-CH ₃
4i	-OCH ₃	-CH ₂ CH ₃
4j	-OCH ₃	-CH ₂ CH=CH ₂
4k	-OCH ₃	-CH ₂ C≡CH
4l	-OCH ₃	-CH(CH ₃) ₂
4m	-OCH ₃	-CH ₂ CH ₂ N(CH ₃) ₂
4n	-OCH ₃	-CH ₂ CH ₂ CH ₂ N(CH ₃) ₂

Scheme 1 Synthesis pathway for obtained compounds.

compounds **3a, 3b** and appropriate piperazine derivatives were reacted to synthesize target compounds (**4a–4n**). The structures of the obtained compounds were proved by $^1\text{H-NMR}$, $^{13}\text{C-NMR}$ and HRMS spectroscopic methods (ESI \ddagger).

When the chemical structures of the synthesized compounds were examined, the specific stretching band of the carbonyl ($\text{C}=\text{O}$) was recorded between 1660 – 1681 cm^{-1} . The $\text{C}=\text{C}$ stretching band on this group was obtained in the range of 1442 – 1473 cm^{-1} . All the synthesis products (**4a–4n**) contain a 1,4-disubstituted benzene ring in their structure. The specific out-of-plane deformation band of this ring was observed in the range of 812 – 871 cm^{-1} .

Aliphatic and aromatic protons in the synthesized compounds gave peaks in the ^1H NMR spectra as expected. In the spectra of the obtained compounds, the total hydrogen number was determined, and the expected number of peaks was observed. In the synthesized compounds, there are two main substructures as non-substituted benzothiazole and 5-



methoxy benzothiazole. When the ^1H NMR results of the derivatives (**4a–4g**) containing the non-substituted benzothiazole structure are examined, the striking details are as follows.

Protons belonging to the benzothiazole substructure in compounds **4a–4g** are a hydrogen triplet (δ_{H} 7.31–7.33 ppm), a hydrogen multiple (δ_{H} 7.42–7.46 ppm), and two hydrogen doublets (δ_{H} 7.76–7.78; 7.99–8.01 ppm). Protons belonging to the 1,4-disubstituted benzene ring were observed as an AB system [δ_{H} 7.40–7.48 (2H); 7.96–8.11 ppm (2H)].

Protons belonging to the 5-methoxybenzothiazole substructure in compounds **4h–4n** are a hydrogen doublet (δ_{H} 6.76–7.07 ppm), a hydrogen doublet (δ_{H} 6.99–7.62 ppm) and a hydrogen doublet (δ_{H} 7.29–7.82 ppm). Protons belonging to the 1,4-disubstituted benzene ring were observed as an AB system [δ_{H} 7.36–7.47 (2H); 7.95–8.10 ppm (2H)].

In the synthesized compounds, the common structural particles gave peaks in the ^{13}C -NMR spectra as expected in general. In the spectra of the compounds, carbons belonging to the carbonyl ($\text{C}=\text{O}$) gave a peak in range of 165.98–166.59 ppm and agreed with the literature data.¹⁸ The other aliphatic carbons were observed in the range of 11.93–79.86 ppm, while aromatic carbons were observed in the range of 102.78–166.59 ppm.

2.2. Cholinesterase enzymes inhibition assay

The inhibitory activities of all obtained derivatives (**4a–4n**) against cholinesterase enzymes were evaluated using the previously described *in vitro* modified Ellman's spectrophotometric method.^{19–27} Activity tests were carried out in two steps. Enzyme inhibition tests were performed by preparing all compounds (**4a–4n**) and reference agents (donepezil and tacrine) at 10^{-3} and 10^{-4} M concentrations. The IC_{50} values of the selected compounds and standard agents were determined by non-linear regression analysis over the calculated % inhibition values at the concentrations between 10^{-3} – 10^{-9} M (by serial dilutions) with the help of *GraphPad Prism Version 6*

software. Enzyme inhibition results, IC_{50} values of test compounds and reference drugs are presented in Table 1 (the IC_{50} curves are presented in ESI, Fig. S53†).

In the enzyme inhibition test, it was observed that all compounds were more effective against AChE at 10^{-3} M concentrations. Also, compounds carrying dimethylaminoethyl and dimethylaminopropyl side chains showed inhibitory activity against AChE comparable to donepezil. Among the compounds, **4a**, **4d**, **4f**, **4g**, **4h**, **4k**, **4m** and **4n** showed more than 50% inhibition at 10^{-4} M concentration. The IC_{50} values of compounds **4a**, **4d**, **4f**, **4g**, **4h**, **4k**, **4m** and **4n** were calculated as 56.3 ± 2.5 nM, 89.6 ± 3.2 nM, 23.4 ± 1.1 nM, 36.7 ± 1.4 nM, 64.9 ± 2.9 nM, 102.5 ± 4.8 nM, 27.8 ± 1.0 nM, and 42.1 ± 1.8 nM, respectively. These compounds came to the fore because they have very close IC_{50} values to that of donepezil. The IC_{50} value of donepezil was found to be 20.1 ± 1.4 nM. Among these derivatives, the **4f** was found to be the most active derivative in the series with an IC_{50} value of 23.4 ± 1.1 nM.

When the BChE inhibition test results were examined, it was observed that the reference compound tacrine had an inhibition activity of $99.8 \pm 1.4\%$ and $98.7 \pm 1.4\%$ at 10^{-3} and 10^{-4} M concentrations, respectively. However, none of the compounds showed significant inhibitory activity against BChE (Table 1).

2.3. MAO enzymes inhibition assay

The inhibition effect of synthesized compounds on MAO isoenzymes was evaluated by using the *in vitro* fluorometric method described previously by our research group.^{28–34} The IC_{50} values of the selected compounds and standard agents were determined by non-linear regression analysis over the calculated % inhibition values at the concentrations between 10^{-3} – 10^{-9} M (by serial dilutions) with the help of *GraphPad Prism Version 6* software. The results are presented in Table 2 and ESI, Fig. S54.† In MAO-A inhibition test, the reference agent moclobemide showed an inhibition of $94.1 \pm 2.8\%$ at 10^{-3} M concentration. However, none of the synthesized compounds

Table 1 % inhibition and IC_{50} values of the synthesized compounds, donepezil and tacrine, against ChE enzymes

Comp.	AChE % inhibition			BChE % inhibition		
	10^{-3} M	10^{-4} M	AChE IC_{50} (nM)	10^{-3} M	10^{-4} M	BChE IC_{50} (nM)
4a	93.3 ± 1.4	89.1 ± 1.1	56.3 ± 2.5	38.6 ± 0.7	26.5 ± 0.8	$>10^6$
4b	85.6 ± 1.3	47.6 ± 0.8	$>10^5$	35.7 ± 0.9	24.4 ± 0.6	$>10^6$
4c	82.8 ± 1.5	48.2 ± 0.9	$>10^5$	30.9 ± 0.7	20.2 ± 0.7	$>10^6$
4d	91.6 ± 1.3	86.5 ± 1.1	89.6 ± 3.2	37.1 ± 0.8	28.4 ± 0.9	$>10^6$
4e	83.9 ± 1.7	46.9 ± 0.8	$>10^5$	39.1 ± 0.8	26.8 ± 0.7	$>10^6$
4f	96.4 ± 1.4	93.0 ± 1.3	23.4 ± 1.1	45.3 ± 0.9	32.8 ± 0.6	$>10^6$
4g	94.3 ± 1.0	90.6 ± 1.3	36.7 ± 1.4	41.5 ± 0.8	30.9 ± 0.8	$>10^6$
4h	92.3 ± 1.1	87.4 ± 1.3	64.9 ± 2.9	33.5 ± 0.8	27.0 ± 0.7	$>10^6$
4i	86.9 ± 1.2	48.0 ± 0.9	$>10^5$	39.8 ± 0.9	25.2 ± 0.9	$>10^6$
4j	82.5 ± 1.5	47.6 ± 0.8	$>10^5$	32.9 ± 0.8	22.6 ± 0.8	$>10^6$
4k	90.3 ± 1.5	84.7 ± 1.3	102.5 ± 4.8	30.4 ± 0.7	26.4 ± 0.7	$>10^6$
4l	81.7 ± 1.3	48.1 ± 0.9	$>10^5$	38.1 ± 0.9	24.3 ± 0.7	$>10^6$
4m	95.3 ± 1.2	91.8 ± 1.3	27.8 ± 1.0	42.4 ± 0.8	31.9 ± 0.8	$>10^6$
4n	95.3 ± 1.7	90.0 ± 1.4	42.1 ± 1.8	40.9 ± 0.9	30.4 ± 0.9	$>10^6$
Donepezil	99.1 ± 1.3	97.4 ± 1.3	20.1 ± 1.4	—	—	—
Tacrine	—	—	—	99.8 ± 1.4	98.7 ± 1.4	6.4 ± 0.2



Table 2 % inhibition and IC₅₀ values of the synthesized compounds, moclobemide and selegiline, against MAO enzymes

Comp	MAO-A % inhibition			MAO-B % inhibition		
	10 ⁻³ M	10 ⁻⁴ M	MAO-A IC ₅₀ (nM)	10 ⁻³ M	10 ⁻⁴ M	MAO-B IC ₅₀ (nM)
4a	55.3 ± 0.9	38.6 ± 0.7	>10 ⁵	91.0 ± 1.1	88.7 ± 1.3	67.4 ± 3.1
4b	46.5 ± 0.8	36.4 ± 0.8	>10 ⁶	73.3 ± 1.2	42.3 ± 0.8	>10 ⁵
4c	48.3 ± 0.9	34.6 ± 0.8	>10 ⁶	69.6 ± 1.2	40.3 ± 0.9	>10 ⁵
4d	57.6 ± 0.9	39.7 ± 0.9	>10 ⁵	89.5 ± 1.2	84.0 ± 1.1	109.7 ± 4.3
4e	44.7 ± 0.9	33.8 ± 0.7	>10 ⁶	72.7 ± 1.1	44.6 ± 0.8	>10 ⁵
4f	67.9 ± 1.1	41.3 ± 0.9	>10 ⁵	95.3 ± 1.3	91.3 ± 1.1	40.3 ± 1.7
4g	64.9 ± 1.1	40.1 ± 0.9	>10 ⁵	74.2 ± 1.0	42.5 ± 0.9	>10 ⁵
4h	60.5 ± 0.9	38.5 ± 0.6	>10 ⁵	90.6 ± 1.4	85.7 ± 1.4	85.1 ± 3.8
4i	43.8 ± 0.9	30.6 ± 0.7	>10 ⁶	75.6 ± 1.2	41.7 ± 0.9	>10 ⁵
4j	45.2 ± 0.9	32.9 ± 0.7	>10 ⁶	74.5 ± 1.1	43.5 ± 0.8	>10 ⁵
4k	58.6 ± 0.9	39.9 ± 0.8	>10 ⁵	88.4 ± 1.5	85.9 ± 1.1	124.3 ± 5.8
4l	40.6 ± 0.9	34.0 ± 0.9	>10 ⁶	77.9 ± 1.4	40.7 ± 0.9	>10 ⁵
4m	61.3 ± 0.9	37.9 ± 0.8	>10 ⁵	93.3 ± 1.3	90.9 ± 1.5	56.7 ± 2.2
4n	60.1 ± 0.8	38.8 ± 0.7	>10 ⁵	70.3 ± 1.3	41.0 ± 0.9	>10 ⁵
Moc.	94.1 ± 2.8	82.1 ± 2.7	6061.3 ± 262.5	—	—	—
Selegilin	—	—	—	98.6 ± 2.1	94.9 ± 1.1	37.4 ± 1.6

(**4a–4n**) showed greater than 50% inhibition in this concentration.

In the MAO-B inhibition test, compounds **4a**, **4d**, **4f**, **4h**, **4k** and **4m** showed more than 50% inhibition at 10⁻³ and 10⁻⁴ M concentrations. Compounds were observed to be more effective on MAO-B compared to MAO-A-A enzyme. The IC₅₀ values of **4a**, **4d**, **4f**, **4h**, **4k** and **4m** were found as 67.4 ± 3.1 nM, 109.7 ± 4.3 nM, 40.3 ± 1.7 nM, 85.1 ± 3.8 nM, 124.3 ± 5.8 nM and 56.7 ± 2.2 nM, respectively. The IC₅₀ value of the reference drug selegiline was calculated as 37.4 ± 1.6 nM. Accordingly, among the synthesized compounds, the **4f** is the most active derivative with the similar IC₅₀ value to that of selegiline. Therefore, the compound **4f**, exhibiting inhibitory activity profile on both AChE and MAO-B enzymes, can be suggested as a dual enzyme inhibitor against AD.

2.4. Inhibition of beta amyloid 1–42 (Aβ42) aggregation

The beta amyloid aggregation inhibitory activities of compounds **4a**, **4d**, **4f**, **4h**, **4k** and **4m**, which show high

inhibitory activity against AChE and MAO-B enzymes, were investigated by using a fluorometric beta amyloid 1–42 (Aβ42) ligand screening assay (BioVision, Milpitas, CA, USA). If an Aβ42 ligand is present by the procedure, this reaction is inhibited/destroyed, thereby reducing or completely eliminating fluorescence. Percent inhibition of beta amyloid 1–42 (Aβ42) peptide aggregation is given in Fig. 2. The compounds were tested at concentrations of 10 μM, 1 μM, 0.1 μM, and 0.01 μM, and the Aβ42 inhibitor included in the kit was used as a standard. All test compound concentrations were applied in quadruplicate in plates.

According to Fig. 2, compounds **4a**, **4d**, **4f**, **4h**, **4k** and **4m**, exhibited greater than 50% inhibition (91.9 ± 3.1%, 89.8 ± 3.0%, 97.3 ± 3.2%, 90.7 ± 2.9%, 87.1 ± 3.2% and 94.7 ± 2.1%, respectively) at 10 μM concentration. They also exhibited more than 50% inhibition at a concentration of 1 μM. They showed inhibition as 86.4 ± 2.7%, 81.5 ± 2.5%, 90.6 ± 3.1%, 83.2 ± 3.3%, 77.7 ± 2.7% and 88.9 ± 2.0%, respectively. Compounds

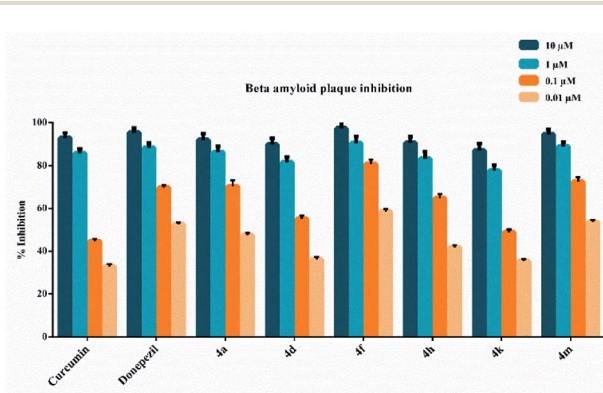


Fig. 2 Beta amyloid plaque inhibition (%) of compounds **4a**, **4d**, **4f**, **4h**, **4k** and **4m**.

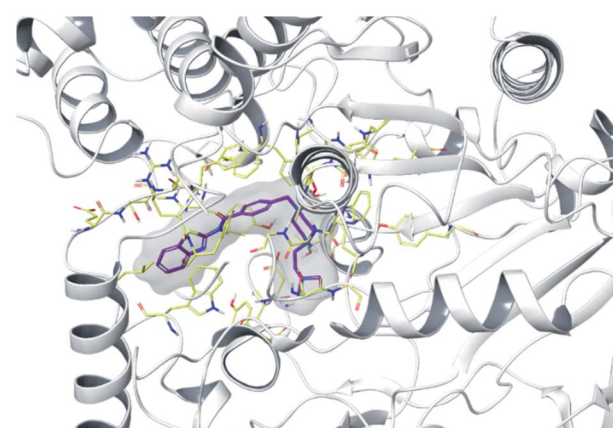


Fig. 3 The localization of compound **4f** to the AChE enzyme active site (PDBID: 4EY7).



4a, 4d, 4f, 4h, 4k and 4m showed inhibition as $70.4 \pm 2.8\%$, $55.2 \pm 1.4\%$, $80.8 \pm 2.1\%$, $64.8 \pm 1.9\%$, $48.9 \pm 1.3\%$ and $72.5 \pm 2.2\%$, respectively at a concentration of $0.1 \mu\text{M}$. Their inhibition potency was $47.4 \pm 1.1\%$, $36.2 \pm 1.0\%$, $58.6 \pm 1.1\%$, $41.8 \pm 1.0\%$, $35.4 \pm 1.0\%$ and $53.6 \pm 1.0\%$, respectively at a concentration of $0.01 \mu\text{M}$. The IC_{50} values of curcumin and donepezil were calculated as $105.5 \pm 4.1 \text{ nM}$ and $236.5 \pm 10.5 \text{ nM}$, respectively. Besides, compounds **4a, 4d, 4f, 4h, 4k** and **4m** displayed IC_{50} values of $256.1 \pm 11.0 \text{ nM}$, $241.8 \pm 9.7 \text{ nM}$, $167.5 \pm 8.0 \text{ nM}$, $295.5 \pm 13.0 \text{ nM}$, $324.7 \pm 15.1 \text{ nM}$ and $198.8 \pm 8.8 \text{ nM}$, respectively. Compounds **4f** and **4m** exhibited a higher inhibition potential compared to compounds **4a, 4d, 4h, and 4k**. As a result, it has been revealed that compounds **4f** and **4m** may have a potential to inhibit AChE and MAO-B enzymes, as well as the ability to prevent the formation of beta amyloid plaques accumulated in the brains of patients suffering from AD.

2.5. Cytotoxicity assay

Compound **4f**, exhibiting potent AchE-MAO-B inhibition profile, were further tested for cytotoxicity against NIH/3T3 cell line by MTT assay and its IC_{50} value was calculated. Compound **4f** showed an IC_{50} value of $72.9 \pm 2.7 \mu\text{M}$ against NIH/3T3 cells. This result suggests that it has not cytotoxic potential at its effective concentrations against AChE and MAO-B enzymes.

2.6. Molecular docking studies on AChE and MAO-B enzymes

To determine the possible interactions of compound **4f**, which has the highest inhibition on AChE and MAO-B enzymes, with the relevant enzyme active sites. Docking studies were carried out on crystal structures of AChE (PDB code: 4EY7)³⁵ and MAO-B (PDB f: 2V5Z)³⁶ enzymes. In the studies, Glide 7.1 (ref. 37) program was used and the most probable poses were produced with GlideScore SP. For validations of docking methods, studies were performed firstly under the same conditions with suitable

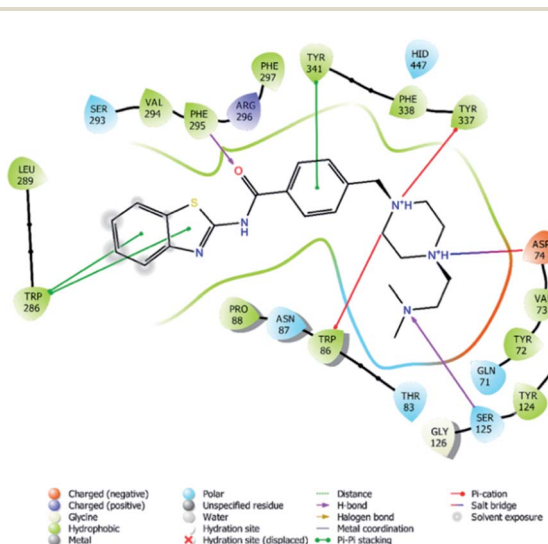


Fig. 4 2D interaction of compound **4f** at binding region of AChE (PDBID: 4EY7).

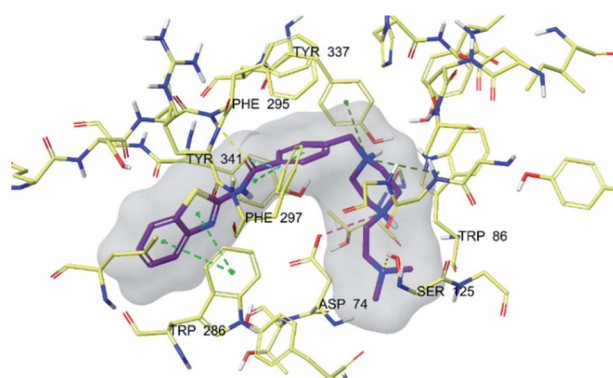


Fig. 5 3D interaction of compound **4f** at binding region of AChE (PBDID: 4EY7). Maroon carbons: compound **4f**; yellow carbons: binding site residues; yellow dashes: H-bond; blue dashes: aromatic H-bond; green dashes: π - π interaction; dark green dashes: π -cation; pink dashes: salt bridge.

ligands. At this step, the obtained compatible interaction results of the reference ligands were compared with the literature. Thus, the docking protocols were confirmed, and further studies were carried out for selected active compound **4f** (the docking poses of reference ligands are presented in ESI, Fig. S52†). Docking poses related to AChE and MAO-B enzyme are given in Fig. 3–5 and Fig. 6–9, respectively.

In many molecular modeling studies, it has been determined that donepezil interacts with both regions of the AChE enzyme and settles very well in the passage with its dual binding site (DBS) feature.^{38–40} Cheung *et al.* (2012) examined the binding sites of donepezil to enzyme active sites and explained the interactions of donepezil with active sites. In the CAS region, the benzyl ring shows π – π interaction with the indole ring of Trp86. The carbonyl group has an important interaction. Hydrogen bonding is established between the carbonyl oxygen of indanone and the amino group of Phe395. In the PAS region, the indanone structure binds with the indole in Trp286 by π – π interaction. In addition, the piperidine ring is in van der Waals interaction with both the CAS and PAS domains.³⁵ The docking study of compound **4f** with the AChE indicates that it bounds

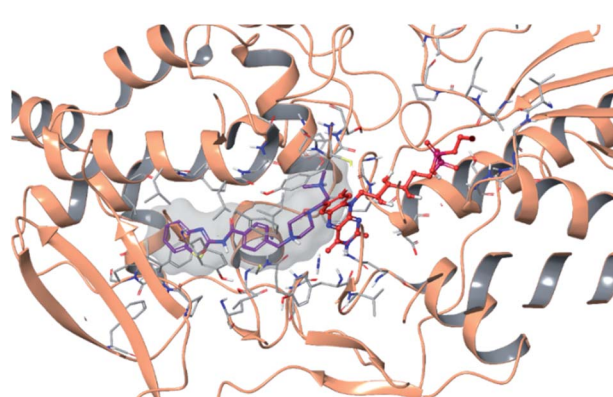


Fig. 6 The localization of compound **4f** to the MAO-B enzyme active site (PDBID: 2V5Z).

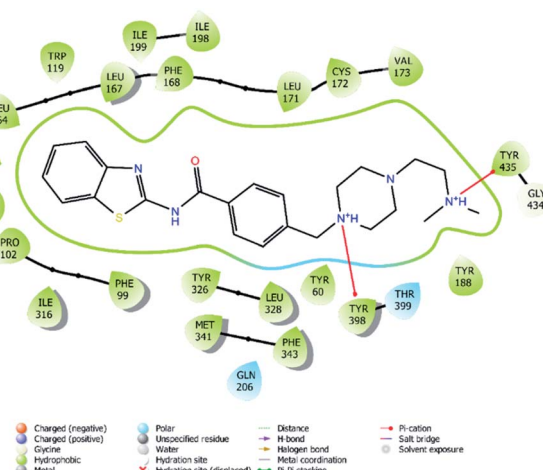


Fig. 7 2D interaction of compound **4f** at binding region of MAO-B (PBDID: 2V5Z).

very strongly to the enzyme active site by forming various interactions. Like donepezil, it is seen that the compound **4f** binds to both the CAS and PAS regions of the enzyme. It settles in the gate and thus can interact fully, taking advantage of the features of the DBS. As can be seen in Fig. 4 and 5, both the phenyl and thiazole parts of the benzothiazole ring in compound **4f** form two π – π interactions with the indole ring of amino acid Trp286. It is seen that carbonyl group is also very important in terms of polar interactions. It forms a hydrogen bond with the amino group of Phe295 and an aromatic–hydrogen bond with the phenyl of Phe297. These interactions of benzothiazole and carbonyl show that compound **4f** strongly settle-downs in the PAS region, as donepezil does. It has been determined that the benzene ring in the middle of the structure forms a π – π interaction with the phenyl of the Tyr341. It is seen that nitrogen atom in the 1st position of piperazine forms two cation– π interactions with the indole of Trp86 and the phenyl of Tyr337. It has been determined that nitrogen atom in the 4th position of piperazine forms a salt bridge with the carbonyl of Asp74. Finally, it has been determined that the terminal

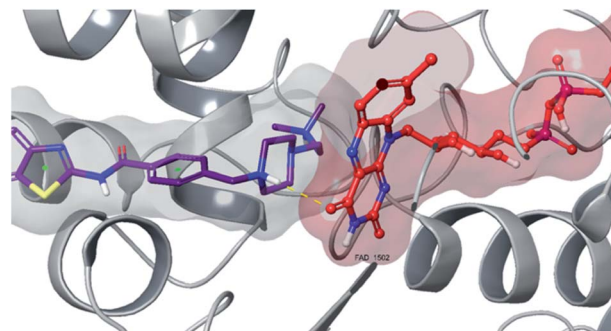


Fig. 9 3D interaction of compound **4f** with FAD at binding region of MAO-B (PBDID: 2V5Z).

nitrogen atom in the dimethylaminoethyl side chain forms a hydrogen bond with the hydroxyl of Ser125. These interactions with Asp74, Trp86, Ser125, Tyr337 and Tyr341 supply very strong and conformable binding to the CAS region of the AChE enzyme active site. All above data explain the strong inhibitory activity of compound **4f** on AChE enzyme *in vitro*.

Structural difference between compounds **4a**–**4g** and **4h**–**4m** is the presence of the methoxy group at 5th position of benzothiazole ring in compounds **4h**–**4m**. Hence, molecular docking studies were carried out with compound **4m**, carrying methoxy substituent, to explain how the inclusion of this group in the structure influenced binding to the AChE enzyme active site. The docking pose of compound **4m** on AChE enzyme was given in ESI, Fig. S51.† According to this docking pose compound **4m** showed the same interactions with Trp286, Phe295 and Tyr341 as explained in interactions for compound **4f**. The presence of methoxy group monopolized the binary π – π interaction with Trp286. At the same time, the Trp86 interaction, which is an important interaction in the CAS region of the enzyme has been lost due to growth in the molecule. The other interactions observed in the docking pose of **4f** could not be identified for compound **4m**. These findings reveal that the methoxy substituent at the 5th position of the benzothiazole ring reduced the binding potency to the active region and also biological activity. It can be suggested that the methoxy effects the conformations of the compounds and thus the derivatives with this moiety show different interactions and less binding profile to enzyme active site.

Fig. 6–8 show the docking poses of compound **4f** with the MAO-B enzyme. As seen in the poses, compound **4f** is strongly and favorably located in the active site of the MAO-B enzyme, as in the AChE enzyme. The benzothiazole ring forms an aromatic–hydrogen bond with the carbonyl of Pro102. It is seen that the terminal nitrogen atom of dimethylaminoethyl side chain establishes a cation– π interaction with the phenyl of Try435. The nitrogen in the 1st position of the piperazine forms the same interaction with the phenyl of Tyr398. In addition, it has been determined that the piperazine ring forms a hydrogen bond with the carbonyl adjacent to the N5 of FAD molecule located in the enzyme active site (see Fig. 6 and 9). This interaction reveals that compound **4f** binds strongly and appropriately to the substrate binding site of MAO-B enzyme active site

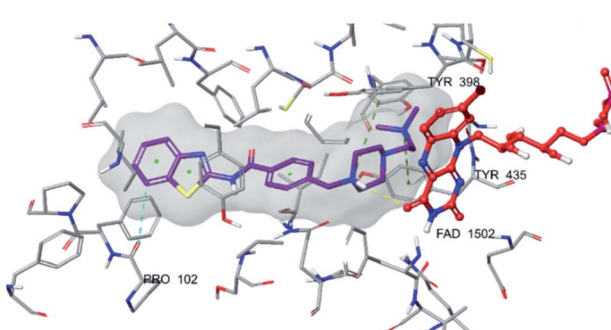


Fig. 8 3D interaction of compound **4f** at binding region of MAO-B (PBDID: 2V5Z). Maroon carbons: compound **4f**; red carbons: FAD protein, grey carbons: binding site residues; yellow dashes: H-bond; blue dashes: aromatic H-bond; green dashes: π – π interaction; dark green dashes: π –cation.



by interacting with FAD. All available data clearly indicate the strong MAO-B enzyme inhibition profile of compound **4f**.

As a result, compound **4f** forms a hydrogen bond with the cofactor FAD at the MAO-B active site, which is a significant reason for inhibitory potential of this compound (Fig. 9).

3. Experimental

3.1. Chemistry

All reagents were purchased from commercial suppliers and were used without further purification. Melting points (M. p.) were determined on the Mettler Toledo-MP90 Melting Point System and were uncorrected. ¹H-NMR (nuclear magnetic resonance) Bruker DPX 300 FT-NMR spectrometer; ¹³C-NMR, Bruker DPX 75 MHz spectrometer (Bruker Bioscience, Billerica, MA, USA). In the ¹H NMR spectra, the splitting patterns were designated as follows: s: singlet; brs: broad singlet; d: doublet; dd: doublet of doublets; t: triplet; m: multiplet; q: quartet. The coupling constants (*J*) were expressed in Hertz (Hz). Mass spectra were recorded on a LCMS-IT-TOF (Shimadzu, Kyoto, Japan) using ESI.

3.1.1. Synthesis of 4-(chloromethyl) benzoyl chloride (1). 4-(Chloromethyl) benzoic acid (10 g) was dissolved in SO₂Cl₂ (10 mL) and the resulting mixture was refluxed. The reaction was terminated by TLC control, SO₂Cl₂ was removed under low pressure and the remaining residue was scraped off.

3.1.2. Synthesis of the 2-aminobenzothiazoles (2a, 2b). Aniline derivatives (0.03 mol) were dissolved in acetic acid, the equivalent amount of potassium thiocyanate (0.03 mol, 2.915 g) was added and then mixture was taken into an ice bath. A solution of bromine (0.04 mol, 2.015 mL) in acetic acid (10 mL) was added dropwise to the reaction medium. After the dropping process was completed, the reaction contents were stirred at 25 °C for 12 hours. Reaction control was provided with TLC application. The reaction contents were poured into iced-water, boiled and the crude product was filtered off.

3.1.2.1. Benzo[d]thiazol-2-amine (2a). Yield: 70%, cream powder. ¹H-NMR (300 MHz, DMSO-*d*₆): δ = 6.99 (1H, t, *J* = 7.5 Hz, benzothiazole), 7.20 (1H, t, *J* = 7.4, benzothiazole), 7.34 (1H, d, *J* = 7.9 Hz, benzothiazole), 7.50 (2H, s, -NH₂), 7.64 (1H, d, *J* = 7.7 Hz, benzothiazole). HRMS (m/z): [M + H]⁺ calcd for C₇H₆N₂S: 151.0324; found 151.0330.

3.1.2.2. 5-Methoxybenzo[d]thiazol-2-amine (2b). Yield: 71%, beige powder. ¹H-NMR (300 MHz, DMSO-*d*₆): δ = 3.72 (3H, s, -OCH₃), 6.79–6.81 (1H, m, benzothiazole), 7.22–7.29 (4H, m, benzothiazole + NH₂). HRMS (m/z): [M + H]⁺ calcd for C₈H₈N₂SO: 181.0430; found 181.0436.

3.1.3. Synthesis of 4-(chloromethyl)-*N*-(5,6-substitutedbenzo[d]thiazol-2-yl)benzamide (3a, 3b). 2-Amino-benzothiazole (0.03 mol) derivatives were dissolved in 10 mL of tetrahydrofuran (THF) and triethylamine (TEA) (0.04 mol, 5.408 mL) was added to this solution. The reaction mixture was taken into an ice bath. A solution of 4-(chloromethyl) benzoyl chloride (0.03 mol, 5.67 g) in THF (10 mL) was added dropwise to the reaction medium. After the dropping process was completed, the reaction contents were stirred at 25 °C for 5 hours. Reaction control was provided with TLC application. After THF was

evaporated under reduced pressure, the crude product was washed with water and recrystallized from ethanol.

3.1.3.1. *N*-(Benzo[d]thiazol-2-yl)-4-(chloromethyl)benzamide (3a).⁴¹ Yield: 81%, beige powder. ¹H-NMR (300 MHz, DMSO-*d*₆): δ = 4.85 (2H, s, -CH₂-), 7.33 (1H, t, *J* = 7.3 Hz, benzothiazole), 7.47 (1H, t, *J* = 7.8 Hz, benzothiazole), 7.62 (2H, d, *J* = 7.1 Hz, 1,4-disubstitutedbenzene), 7.79 (1H, d, *J* = 7.9 Hz, benzothiazole), 8.02 (1H, d, *J* = 7.9 Hz, benzothiazole), 8.14 (2H, d, *J* = 7.0 Hz, 1,4-disubstitutedbenzene), 12.97 (1H, s, -NH). HRMS (m/z): [M + H]⁺ calcd for C₁₅H₁₁N₂SOCl: 303.0353; found 303.0348.

3.1.3.2. 4-(Chloromethyl)-*N*-(5-methoxybenzo[d]thiazol-2-yl)benzamide (3b). Yield: 79%, beige powder. ¹H-NMR (300 MHz, DMSO-*d*₆): δ = 3.82 (3H, s, -OCH₃), 4.86 (2H, s, -CH₂-), 7.06 (1H, dd, *J*₁ = 2.3 Hz, *J*₂ = 8.6 Hz, benzothiazole), 7.59–7.63 (3H, m, benzothiazole + 1,4-disubstitutedbenzene), 7.68 (1H, d, *J* = 8.8 Hz, benzothiazole), 8.12 (2H, d, *J* = 8.1 Hz, 1,4-disubstitutedbenzene). HRMS (m/z): [M + H]⁺ calcd for C₁₆H₁₃N₂SO₂Cl: 333.0459; found 333.0464.

3.1.4. Synthesis of target compounds (4a–4n).⁴² 4-(Chloromethyl)-*N*-(5,6-substitutedbenzo[d]thiazol-2-yl)benzamide (2 mmol) was dissolved in acetone. After adding the appropriate piperazine derivative (2 mmol) and potassium carbonate (2 mmol, 0.276 g), the solution was refluxed for 12 hours. Reaction control was done by TLC application. Acetone was evaporated under reduced pressure. The crude product was washed with water and recrystallized from ethanol.

3.1.4.1. *N*-(Benzo[d]thiazol-2-yl)-4-((4-methylpiperazine-1-yl)methyl)benzamide (4a). Yield: 87%, cream powder. M. P. = 145.3–147.0 °C. ¹H-NMR (300 MHz, DMSO-*d*₆): δ = 2.14 (3H, s, -CH₃), 2.36 (8H, br.s, piperazine), 3.52 (2H, s, -CH₂-), 7.32 (1H, t, *J* = 4.03 Hz, benzothiazole), 7.43–7.44 (1H, m, benzothiazole), 7.46 (2H, d, *J* = 6.82 Hz, 1,4-disubstitutedbenzene), 7.77 (1H, d, *J* = 7.92 Hz, benzothiazole), 8.00 (1H, d, *J* = 7.56 Hz, benzothiazole), 8.11 (2H, d, *J* = 8.26 Hz, 1,4-disubstitutedbenzene). ¹³C-NMR (75 MHz, DMSO-*d*₆): δ = 46.14, 53.04, 55.14, 62.01, 120.68, 122.16, 124.00, 126.56, 128.78, 129.23, 131.25, 132.00, 144.16, 148.81, 159.76, 166.42. HRMS (m/z): [M + H]⁺ calcd for C₂₂H₂₂N₂O₂: 367.1587; found 367.1595.

3.1.4.2. *N*-(Benzo[d]thiazol-2-yl)-4-((4-ethylpiperazine-1-yl)methyl)benzamide (4b). Yield: 85%, beige powder. M. P. = 149.9–151.9 °C. ¹H-NMR (300 MHz, DMSO-*d*₆): δ = 0.97 (3H, t, *J* = 7.14 Hz, -CH₃), 2.27–2.38 (10H, m, piperazine + -CH₂-), 3.54 (2H, s, -CH₂-), 7.33 (1H, t, *J* = 7.55 Hz, benzothiazole), 7.43–7.46 (1H, m, benzothiazole), 7.47 (2H, d, *J* = 7.95 Hz, 1,4-disubstitutedbenzene), 7.78 (1H, d, *J* = 7.99 Hz, benzothiazole), 8.01 (1H, d, *J* = 7.95 Hz, benzothiazole), 8.11 (2H, d, *J* = 8.18 Hz, 1,4-disubstitutedbenzene). ¹³C-NMR (75 MHz, DMSO-*d*₆): δ = 12.45, 52.06, 52.82, 53.18, 62.03, 120.71, 122.19, 124.06, 126.60, 128.78, 129.24, 131.14, 131.97, 144.23, 148.77, 159.62, 166.37. HRMS (m/z): [M + H]⁺ calcd for C₂₁H₂₄N₄OS: 381.1744; found 381.1754.

3.1.4.3. 4-((4-Allylpiperazine-1-yl)methyl)-*N*-(benzo[d]thiazol-2-yl)benzamide (4c). Yield: 81%, yellow powder. M. P. = 150.1–152.3 °C. ¹H-NMR (300 MHz, DMSO-*d*₆): δ = 2.38 (8H, br.s, piperazine), 2.92 (2H, d, *J* = 6.36 Hz, -CH₂-), 3.54 (2H, s, -CH₂-), 5.08–5.18 (2H, m, -CH₂), 5.72–5.84 (1H, m, CH), 7.31 (1H, t, *J* = 4.03 Hz, benzothiazole), 7.42–7.45 (1H, m, benzothiazole), 7.46



(2H, d, J = 8.24 Hz, 1,4-disubstitutedbenzene), 7.76 (1H, d, J = 7.86 Hz, benzothiazole), 7.99 (1H, d, J = 7.95 Hz, benzothiazole), 8.11 (2H, d, J = 8.25 Hz, 1,4-disubstitutedbenzene). ^{13}C -NMR (75 MHz, DMSO- d_6): δ = 53.04, 53.15, 61.34, 62.04, 117.85, 120.61, 122.13, 123.88, 126.50, 128.78, 129.19, 131.52, 132.05, 136.08, 144.03, 148.89, 160.08, 166.59. HRMS (m/z): [M + H]⁺ calcd for C₂₂H₂₄N₄OS: 393.1744; found 393.1754.

3.1.4.4. *N*-(*Benzod*[*d*]thiazol-2-yl)-4-((4-(*prop*-2-*yn*-1-*yl*)piperazine-1-*yl*)methyl)benzamide (4d). Yield: 79%, cream powder. M. P. = 134.7–136.2 °C. ^1H -NMR (300 MHz, DMSO- d_6): δ = 2.41 (4H, br.s., piperazine), 2.47 (4H, br.s., piperazine), 3.14 (1H, s, -CH), 3.25 (2H, s, -CH₂), 3.54 (2H, s, -CH₂), 7.31 (1H, t, J = 4.03 Hz, benzothiazole), 7.43 (1H, br.s., benzothiazole), 7.47 (2H, d, J = 7.63 Hz, 1,4-disubstitutedbenzene), 7.76 (1H, d, J = 7.89 Hz, benzothiazole), 7.99 (1H, d, J = 7.96 Hz, benzothiazole), 8.11 (2H, d, J = 8.24 Hz, 1,4-disubstitutedbenzene). ^{13}C -NMR (75 MHz, DMSO- d_6): δ = 46.43, 51.60, 53.00, 61.97, 76.12, 79.86, 120.67, 122.14, 123.99, 126.56, 128.80, 129.21, 131.31, 132.00, 144.12, 148.79, 159.78, 166.47. HRMS (m/z): [M + H]⁺ calcd for C₂₂H₂₂N₄OS: 391.1587; found 391.1599.

3.1.4.5. *N*-(*Benzod*[*d*]thiazol-2-yl)-4-((4-isopropylpiperazine-1-*yl*)methyl)benzamide (4e). Yield: 82%, cream powder. M. P. = 140.3–142.0 °C. ^1H -NMR (300 MHz, DMSO- d_6): δ = 1.07 (6H, d, J = 6.51 Hz, -CH₃ + -CH₃), 2.48 (4H, br.s., piperazine), 2.55 (1H, br.s., piperazine), 2.61–2.74 (1H, m, -CH), 3.54 (2H, s, -CH₂), 7.26–7.32 (3H, m, benzothiazole), 7.40 (2H, d, J = 8.16 Hz, 1,4-disubstitutedbenzene), 7.84–7.87 (1H, m, benzothiazole), 7.96 (2H, d, J = 8.29 Hz, 1,4-disubstitutedbenzene). ^{13}C -NMR (75 MHz, DMSO- d_6): δ = 18.65, 48.60, 53.42, 54.45, 62.50, 120.64, 121.42, 123.92, 126.06, 127.93, 129.56, 130.68, 131.97, 144.26, 147.84, 159.68, 165.79. HRMS (m/z): [M + H]⁺ calcd for C₂₂H₂₆N₄OS: 395.1900; found 395.1912.

3.1.4.6. *N*-(*Benzod*[*d*]thiazol-2-yl)-4-((4-(2-(dimethylamino)ethyl)piperazine-1-*yl*)methyl)benzamide (4f). Yield: 78%, yellow powder. M. P. = 175.7–177.2 °C. ^1H -NMR (300 MHz, DMSO- d_6): δ = 2.25 (6H, s, -CH₃ + -CH₃), 2.46 (4H, br.s., piperazine), 2.48 (4H, br.s., piperazine), 2.89 (2H, s, -CH₂), 2.96 (2H, s, -CH₂), 3.54 (2H, s, -CH₂), 7.27–7.30 (2H, m, benzothiazole), 7.37–7.40 (1H, m, benzothiazole), 7.41 (2H, d, J = 8.30 Hz, 1,4-disubstitutedbenzene), 7.84–7.87 (1H, m, benzothiazole), 7.96 (2H, d, J = 8.23 Hz, 1,4-disubstitutedbenzene). ^{13}C -NMR (75 MHz, DMSO- d_6): δ = 45.90, 45.94, 53.03, 53.59, 56.65, 56.89, 62.45, 120.69, 121.42, 123.91, 126.04, 127.91, 129.50, 130.71, 132.02, 144.94, 147.94, 159.49, 165.68. HRMS (m/z): [M + H]⁺ calcd for C₂₃H₂₉N₅OS: 424.2166; found 424.2167.

3.1.4.7. *N*-(*Benzod*[*d*]thiazol-2-yl)-4-((4-(3-(dimethylamino)propyl)piperazine-1-*yl*)methyl)benzamide (4g). Yield: 85%, light brown powder. M. P. = 72.9–74.4 °C. ^1H -NMR (300 MHz, DMSO- d_6): δ = 1.48–1.56 (2H, m, -CH₂–), 2.13 (6H, s, -CH₃ + -CH₃), 2.20–2.27 (4H, m, piperazine), 2.35 (8H, br.s., -CH₂– + -CH₂– + piperazine), 3.52 (2H, s, -CH₂–), 7.31 (1H, t, J = 7.57 Hz, benzothiazole), 7.42–7.44 (1H, m, benzothiazole), 7.45 (2H, d, J = 8.11 Hz, 1,4-disubstitutedbenzene), 7.76 (1H, d, J = 7.95 Hz, benzothiazole), 7.99 (1H, d, J = 7.64 Hz, benzothiazole), 8.11 (2H, d, J = 8.20 Hz, 1,4-disubstitutedbenzene). ^{13}C -NMR (75 MHz, DMSO- d_6): δ = 24.67, 45.40, 53.17, 53.26, 56.35, 57.60, 62.04, 120.64, 122.15, 123.94, 126.54, 128.77, 129.23, 131.37,

132.01, 144.06, 148.84, 159.94, 166.51. HRMS (m/z): [M + H]⁺ calcd for C₂₄H₃₁N₅OS: 438.2322; found 438.2333.

3.1.4.8. *N*-(5-Methoxybenzo[d]thiazol-2-yl)-4-((4-methylpiperazine-1-*yl*)methyl)benzamide (4h). Yield: 85%, light brown powder. M. P. = 137.1–138.9 °C. ^1H -NMR (300 MHz, DMSO- d_6): δ = 2.31 (3H, s, -CH₃), 2.47 (8H, br.s., piperazine), 3.54 (2H, s, -CH₂–), 3.87 (3H, s, -CH₃–), 6.86 (1H, dd, J = 3.82 Hz, benzothiazole), 7.20 (1H, d, J = 8.89 Hz, benzothiazole), 7.32 (1H, d, J = 2.51 Hz, benzothiazole), 7.41 (2H, d, J = 8.27 Hz, 1,4-disubstitutedbenzene), 7.95 (2H, d, J = 8.29 Hz, 1,4-disubstitutedbenzene). ^{13}C -NMR (75 MHz, DMSO- d_6): δ = 46.02, 52.91, 55.06, 55.99, 61.93, 105.09, 105.95, 113.32, 115.51, 118.52, 121.45, 128.71, 129.28, 144.13, 154.70, 156.69, 165.16. HRMS (m/z): [M + H]⁺ calcd for C₂₁H₂₄N₄O₂S: 397.1693; found 397.1707.

3.1.4.9. 4-((4-Ethylpiperazine-1-*yl*)methyl)-N-(5-methoxybenzo[d]thiazol-2-yl)benzamide (4i). Yield: 87%, dark brown powder. M. P. = 129.8–130.9 °C. ^1H -NMR (300 MHz, DMSO- d_6): δ = 1.11 (3H, t, J = 7.17 Hz, -CH₃), 2.41–2.48 (10H, m, -CH₂– + piperazine), 3.55 (2H, s, -CH₂–), 3.87 (3H, s, -CH₃–), 6.83 (1H, dd, J_1 = 3.63 Hz, J_2 = 9.0 Hz, benzothiazole), 7.13 (1H, d, J = 8.83 Hz, benzothiazole), 7.31 (1H, d, J = 2.13 Hz, benzothiazole), 7.40 (2H, d, J = 7.96 Hz, 1,4-disubstitutedbenzene), 7.95 (2H, d, J = 8.00 Hz, 1,4-disubstitutedbenzene). ^{13}C -NMR (75 MHz, DMSO- d_6): δ = 11.93, 52.31, 52.71, 53.05, 55.79, 62.46, 103.88, 115.24, 121.29, 127.94, 129.51, 130.78, 133.20, 142.00, 144.15, 156.75, 157.67, 165.63. HRMS (m/z): [M + H]⁺ calcd for C₂₂H₂₆N₄O₂S: 411.1849; found 411.1854.

3.1.4.10. 4-((4-Allylpiperazine-1-*yl*)methyl)-N-(5-methoxybenzo[d]thiazol-2-yl)benzamide (4j). Yield: 90%, brown powder. M. P. = 173.9–175.5 °C. ^1H -NMR (300 MHz, DMSO- d_6): δ = 2.38 (8H, piperazine), 2.92 (2H, d, J = 6.34 Hz, -CH₂–), 3.54 (2H, s, -CH₂–), 3.83 (3H, s, -CH₃–), 5.09–5.19 (2H, m, -CH₂), 5.75–5.84 (1H, m, -CH–), 7.07 (1H, dd, J_1 = 3.82 Hz, J_2 = 6.0 Hz, benzothiazole), 7.47 (2H, d, J = 8.41 Hz, 1,4-disubstitutedbenzene), 7.62 (1H, d, J = 2.57 Hz, benzothiazole), 7.68 (1H, d, J = 8.82 Hz, benzothiazole), 8.10 (2H, d, J = 8.26 Hz, 1,4-disubstitutedbenzene). ^{13}C -NMR (75 MHz, DMSO- d_6): δ = 53.07, 54.85, 55.57, 57.03, 61.99, 104.02, 106.13, 116.50, 120.35, 122.50, 127.63, 130.32, 131.06, 135.03, 137.04, 142.93, 144.13, 157.33, 165.94. HRMS (m/z): [M + H]⁺ calcd for C₂₃H₂₆N₄O₂S: 423.1849; found 423.1860.

3.1.4.11. *N*-(5-Methoxybenzo[d]thiazol-2-yl)-4-((4-(*prop*-2-*yn*-1-*yl*)piperazine-1-*yl*)methyl)benzamide (4k). Yield: 86%, brown powder. M. P. = 99.9–101.8 °C. ^1H -NMR (300 MHz, DMSO- d_6): δ = 2.49 (4H, br.s., piperazine), 2.59 (4H, br.s., piperazine), 2.93 (1H, d, J = 21.96 Hz, -CH), 3.32 (2H, s, -CH₂–), 36.53 (2H, s, -CH₂–), 3.86 (3H, s, -CH₃), 6.79 (1H, dd, J = 3.79 Hz, J_2 = 9.0 Hz, benzothiazole), 7.06 (1H, d, J = 8.89 Hz, benzothiazole), 7.30 (1H, d, J = 2.49 Hz, benzothiazole), 7.38 (2H, d, J = 8.22 Hz, 1,4-disubstitutedbenzene), 7.95 (2H, d, J = 8.24 Hz, 1,4-disubstitutedbenzene). ^{13}C -NMR (75 MHz, DMSO- d_6): δ = 46.80, 51.83, 52.91, 52.96, 54.81, 62.35, 71.62, 102.78, 103.83, 115.21, 121.22, 122.30, 128.05, 129.42, 141.90, 144.04, 156.73, 157.96, 165.87. HRMS (m/z): [M + H]⁺ calcd for C₂₃H₂₄N₄O₂S: 421.1693; found 421.1693.

3.1.4.12. 4-((4-Isopropylpiperazine-1-*yl*)methyl)-N-(5-methoxybenzo[d]thiazol-2-yl)benzamide (4l). Yield: 89%, brown powder. M. P. = 126.3–128.1 °C. ^1H -NMR (300 MHz, DMSO- d_6):



$\delta = 1.05$ (5H, d, $J = 6.52$ Hz, $-\text{CH}_3 + -\text{CH}_3$), 2.46 (4H, br.s., piperazine), 2.53 (4H, br.s., piperazine), 2.61–2.69 (1H m, $-\text{CH}$), 3.51 (2H, s, $-\text{CH}_2-$), 3.85 (3H, s, $-\text{CH}_3$), 6.76 (1H, dd, $J_1 = 3.82$ Hz, $J_2 = 9.0$ Hz, benzothiazole), 6.99 (1H, d, $J = 8.90$ Hz, benzothiazole), 7.29 (1H, d, $J = 2.47$ Hz, benzothiazole), 7.36 (2H, d, $J = 8.26$ Hz, 1,4-disubstitutedbenzene), 7.95 (2H, d, $J = 8.29$ Hz, 1,4-disubstitutedbenzene). ^{13}C -NMR (75 MHz, DMSO- d_6): $\delta = 18.66, 48.59, 53.46, 54.43, 55.71, 55.76, 62.53, 103.76, 115.22, 121.20, 128.20, 129.53, 130.85, 133.10, 141.84, 144.07, 156.69, 158.10, 165.98$. HRMS (m/z): [M + H]⁺ calcd for $\text{C}_{23}\text{H}_{28}\text{N}_4\text{O}_2\text{S}$: 425.2006; found 425.2013.

3.1.4.13. 4-((4-(2-(Dimethylamino)ethyl)piperazine-1-yl)methyl)-N-(5-methoxybenzo[d]thiazol-2-yl)benzamide (**4m**). Yield: 81%, orange powder. M. P. = 60.1–62.0 °C. ^1H -NMR (300 MHz, DMSO- d_6): $\delta = 2.15$ (6H, s, $-\text{CH}_3 + -\text{CH}_3$), 2.36–2.52 (10H, m, piperazine + $-\text{CH}_2-$), 3.45 (2H, t, $J = 3.45$ Hz, $-\text{CH}_2-$), 3.53 (2H, s, $-\text{CH}_2-$), 3.83 (3H, s, $-\text{CH}_3$), 7.06 (1H, dd, $J_1 = 3.81$ Hz, $J_2 = 9.0$ Hz, benzothiazole), 7.47 (2H, d, $J = 8.28$ Hz, 1,4-disubstitutedbenzene), 7.61 (1H, d, $J = 2.56$ Hz, benzothiazole), 7.68 (2H, d, $J = 8.83$ Hz, benzothiazole), 8.10 (2H, d, $J = 8.29$ Hz, 1,4-disubstitutedbenzene). ^{13}C -NMR (75 MHz, DMSO- d_6): $\delta = 45.83, 45.87, 53.15, 53.53, 56.15, 56.84, 62.02, 120.32, 121.39, 127.61, 128.69, 129.24, 131.22, 133.33, 142.99, 144.03, 156.62, 157.54, 166.06$. HRMS (m/z): [M + H]⁺ calcd for $\text{C}_{24}\text{H}_{31}\text{N}_5\text{O}_2\text{S}$: 454.2271; found 454.2280.

3.1.4.14. 4-((4-(3-(Dimethylamino)propyl)piperazine-1-yl)methyl)-N-(5-methoxybenzo[d]thiazol-2-yl)benzamide (**4n**). Yield: 83%, brown powder. M. P. = 137.3–139.1 °C. ^1H -NMR (300 MHz, DMSO- d_6): $\delta = 1.47$ –1.57 (2H, m, $-\text{CH}_2-$), 2.12 (6H, s, $-\text{CH}_3 + -\text{CH}_3$), 2.19 (2H, t, $J = 6.60$ Hz, $-\text{CH}_2-$), 2.24 (2H, t, $J = 3.66$ Hz, $-\text{CH}_2-$), 2.37 (8H, br.s., piperazine), 3.53 (2H, s, $-\text{CH}_2-$), 3.83 (3H, s, $-\text{CH}_3$), 7.06 (1H, dd, $J_1 = 3.81$ Hz, $J_2 = 9.0$ Hz, benzothiazole), 7.46 (2H, d, $J = 8.27$ Hz, 1,4-disubstitutedbenzene), 7.61 (1H, d, $J = 2.55$ Hz, benzothiazole), 7.67 (1H, d, $J = 8.83$ Hz, benzothiazole), 8.10 (2H, d, $J = 8.26$ Hz, 1,4-disubstitutedbenzene). ^{13}C -NMR (75 MHz, DMSO- d_6): $\delta = 24.80, 45.49, 53.18, 53.27, 56.04, 56.41, 57.67, 62.04, 105.05, 115.40, 121.36, 128.69, 129.22, 131.30, 133.35, 143.02, 143.99, 156.60, 157.66, 166.09$. HRMS (m/z): [M + H]⁺ calcd for $\text{C}_{25}\text{H}_{33}\text{N}_5\text{O}_2\text{S}$: 468.2428; found 468.2436.

3.2. Cholinesterase enzymes inhibition assay

The *in vitro* AChE and BChE inhibition potencies of the synthesized compounds (**4a–4n**) were evaluated according to the modified Ellman's spectrophotometric method.²⁰ The reagents and materials used in the enzyme inhibition assay were supplied commercially by Sigma-Aldrich (St Louis, MO, USA) and Fluka (Steinheim, Germany). The cholinesterase enzyme inhibition procedure was applied as reported in our previous research papers.^{19,21–27} Human acetylcholinesterase (CAS no.: 9000-81-1) and human butyrylcholinesterase (CAS no.: 9001-08-5) enzymes were used as enzymes.

3.3. MAO enzymes inhibition assay

The *in vitro* MAO inhibition test was performed using the available fluorometric method and the percentages and IC_{50}

values of obtained compounds were calculated as previously described by our research group.^{28–34}

3.4. Inhibition of beta amyloid 1–42 (A β 42) aggregation

The test procedure was created based on the protocol of the beta amyloid 1–42 (A β 42) ligand screening assay (BioVision, Milpitas, CA, USA), based on the fluorometric method.

3.5. Cytotoxicity assay

The NIH/3T3 mouse embryonic fibroblast cell line (ATCC® CRL-1658™, London, UK) was used for cytotoxicity assays. The incubation period of NIH/3T3 cells was based on the supplier's recommendation. NIH/3T3 cells were seeded at 1×10^4 cells into each well of 96-well plates. MTT assay was carried out in accordance with the standards previously described.^{19,21}

3.6. Molecular docking

Molecular docking studies were performed using an *in silico* procedure to define the binding modes of active compound in the active regions of AChE and MAO-B. X-ray crystal structures of the AChE (PDB ID: 4EY7)³⁵ and MAO-B (PDB ID: 2V5Z)⁴³ were retrieved from the Protein Data Bank server (<https://www.pdb.org>, accessed 01 May 2021). The structures of the enzymes were built using the Schrödinger Maestro⁴⁴ interface and were then submitted to the Protein Preparation Wizard protocol of the Schrödinger Suite 2020. The ligand was prepared using the LigPrep module⁴⁵ to correctly assign the protonation states as well as the atom types. Bond orders were assigned, and hydrogen atoms were added to the structures. The grid generation was performed using the Glide module,³⁷ and docking runs were conducted in standard precision (SP) docking mode.

4. Conclusion

In this study, compounds **4a–4n** were synthesized and screened for potential inhibitory activities against AChE, BChE, MAO-A, and MAO-B enzymes. As a result of the studies, compound **4f** showed significant inhibition on AChE and MAO-B enzymes. The IC_{50} value of donepezil was found to be 20.1 ± 1.4 nM against AChE, whereas IC_{50} value of the most active compound **4f** was determined as 23.4 ± 1.1 nM. In other words, it showed activity comparable to donepezil. Additionally, the IC_{50} value of the reference drug selegiline on MAO-B enzyme was calculated as 37.4 ± 1.6 nM. Accordingly, among the synthesized compounds, the most active compound **4f** displayed similar IC_{50} value (40.3 ± 1.7 nM) to that of selegiline. Moreover, β -amyloid 1–42 (A β 42) inhibitor screening studies were performed for active compounds. As a result of these studies, it was observed that especially compound **4f** and **4m** are important agents for dual-acting drug design by inhibiting β -amyloid plaque formation in addition to AChE and MAO-B enzyme inhibitions. Data of molecular docking studies expressed the significant interactions with AChE and MAO-B enzymes, and thus supported the *in vitro* dual inhibitory property of compound **4f**. The findings show that compound **4f** has



a promising potential in the treatment of AD and PD with its dual inhibition profile.

Author contributions

Conceptualization, S. K., D. O., and Z. A. K.; methodology, S. K., D. O., B. N. S. and S. L.; software, D. O. and B. N. S.; validation, D. O. and B. N. S.; formal analysis, D. O. and S. L.; investigation, S. K., B. N. S., D. O., S. L., S. I. and Z. A. K.; resources, Y. Ö., A. Ç. K., Z. A. K. and N. G. K.; data curation, S. K., D. O. and B. N. S.; writing-original draft preparation, S. K., D. O., B. N. S., S. L., S. I., Y. Ö., A. Ç. K., Z. A. K. and N. G. K.; writing-review and editing, B. N. S., D. O. and Y. Ö.; visualization, D. O. and Z. A. K.; supervision, Y. Ö., A. Ç. K., Z. A. K. and N. G. K.; project administration, S. K.; D. O., B. N. S. Y. Ö.; funding acquisition, B. N. S. All authors have read and agreed to the published version of the manuscript.

Conflicts of interest

The authors declare no conflict of interest.

Acknowledgements

This study was supported by Anadolu University Scientific Research Projects Commission under the grant no: 2101S001. As the authors of this study, we thank Anadolu University Faculty of Pharmacy Central Analysis Laboratory for their support and contributions.

References

- Ü. D. Özkay, O. D. Can, Y. Özkay and Y. Özturk, *Pharmacol. Rep.*, 2012, **64**, 834–847.
- T. Liu, S. Chen, J. Du, S. Xing, R. Li and Z. Li, *Eur. J. Med. Chem.*, 2021, 113973.
- G. F. Makhaeva, S. V. Lushchekina, N. V. Kovaleva, T. Y. Astakhova, N. P. Boltneva, E. V. Rudakova, O. G. Serebryakova, A. N. Proshin, I. V. Serkov and T. P. Trofimova, *Bioorg. Chem.*, 2021, **112**, 104974.
- B. Ren, C. Guo, R.-Z. Liu, Z.-Y. Bian, R.-C. Liu, L.-F. Huang and J.-J. Tang, *Eur. J. Med. Chem.*, 2022, **228**, 114031.
- P. H. Syaifie, A. W. Hemasita, D. W. Nugroho, E. Mardliyati and I. Anshori, 2021.
- N. Dunn, G. Pearce and S. Shakir, *J. Psychopharmacol.*, 2000, **14**, 406–408.
- M. Hashimoto, T. Imamura, S. Tanimukai, H. Kazui and E. Mori, *Lancet*, 2000, **356**, 568.
- M. M. Carrasco, L. Agüera, P. Gil, A. Morínigo and T. Leon, *Alzheimer Dis. Assoc. Disord.*, 2011, **25**, 333–340.
- H.-C. Li, K.-X. Luo, J.-S. Wang and Q.-X. Wang, *Medicine*, 2020, **99**, 19443.
- Z. Zhang, J. Guo, M. Cheng, W. Zhou, Y. Wan, R. Wang, Y. Fang, Y. Jin, J. Liu and S.-S. Xie, *Eur. J. Med. Chem.*, 2021, **213**, 113154.
- G. F. Makhaeva, N. V. Kovaleva, N. P. Boltneva, S. V. Lushchekina, E. V. Rudakova, T. S. Stupina, A. A. Terentiev, I. V. Serkov, A. N. Proshin and E. V. Radchenko, *Bioorg. Chem.*, 2020, **94**, 103387.
- R. K. P. Tripathi and S. R. Ayyannan, *Med. Res. Rev.*, 2019, **39**, 1603–1706.
- A. Kumar and A. K. Mishra, *Mini-Rev. Med. Chem.*, 2021, **21**, 314–335.
- E. A. Abd El-Meguid, A. M. Naglah, G. O. Moustafa, H. M. Awad and A. M. El Kerdawy, *Bioorg. Med. Chem. Lett.*, 2022, 128529.
- A. Catalano, A. Rosato, L. Salvagno, D. Iacopetta, J. Ceramella, G. Fracchiolla, M. S. Sinicropi and C. Franchini, *Antibiotics*, 2021, **10**, 803.
- A. Doble, *Neurology*, 1996, **47**, 233S–241S.
- A. D. Cohen and W. E. Klunk, *Neurobiol. Dis.*, 2014, **72**, 117–122.
- A. U. Baran, *Turk. J. Chem.*, 2013, **37**, 927–935.
- B. N. Sağlık, S. İlgin and Y. Özkay, *Eur. J. Med. Chem.*, 2016, **124**, 1026–1040.
- G. L. Ellman, K. D. Courtney, V. Andres Jr and R. M. Featherstone, *Biochem. Pharmacol.*, 1961, **7**, 88–95.
- Ü. D. Özkay, Ö. D. Can, B. N. Sağlık, U. A. Çevik, S. Levent, Y. Özkay, S. İlgin and Ö. Atlı, *Bioorg. Med. Chem. Lett.*, 2016, **26**, 5387–5394.
- U. Acar Çevik, S. Levent, B. Nurpelin Sağlık, Y. Özkay and Z. Asım Kaplancıklı, *Lett. Drug Des. Discovery*, 2017, **14**, 528–539.
- S. Levent, U. Acar Çevik, B. N. Sağlık, Y. Özkay, Ö. D. Can, Ü. D. Özkay and Ü. Uçucu, *Phosphorus, Sulfur Silicon Relat. Elem.*, 2017, **192**, 469–474.
- W. Hussein, B. N. Sağlık, S. Levent, B. Korkut, S. İlgin, Y. Özkay and Z. A. Kaplancıklı, *Molecules*, 2018, **23**, 2033.
- U. Acar Çevik, B. N. Saglik, S. Levent, D. Osmaniye, B. Kaya Çavuşoğlu, Y. Ozkay and Z. A. Kaplancıklı, *Molecules*, 2019, **24**, 861.
- D. Osmaniye, B. N. Sağlık, U. Acar Çevik, S. Levent, B. Kaya Çavuşoğlu, Y. Özkay, Z. A. Kaplancıklı and G. Turan, *Molecules*, 2019, **24**, 2392.
- F. Tok, B. Koçyiğit-Kaymakçıoğlu, B. N. Sağlık, S. Levent, Y. Özkay and Z. A. Kaplancıklı, *Bioorg. Chem.*, 2019, **84**, 41–50.
- B. N. Sağlık, B. K. Çavuşoğlu, D. Osmaniye, S. Levent, U. A. Çevik, S. İlgin, Y. Özkay, Z. A. Kaplancıklı and Y. Öztürk, *Bioorg. Chem.*, 2019, **85**, 97–108.
- Ö. D. Can, D. Osmaniye, Ü. D. Özkay, B. N. Sağlık, S. Levent, S. İlgin, M. Baysal, Y. Özkay and Z. A. Kaplancıklı, *Eur. J. Med. Chem.*, 2017, **131**, 92–106.
- N. Ö. Can, D. Osmaniye, S. Levent, B. N. Sağlık, B. Korkut, Ö. Atlı, Y. Özkay and Z. A. Kaplancıklı, *Eur. J. Med. Chem.*, 2018, **144**, 68–81.
- S. İlgin, D. Osmaniye, S. Levent, B. N. Sağlık, U. Acar Çevik, B. K. Çavuşoğlu, Y. Özkay and Z. A. Kaplancıklı, *Molecules*, 2017, **22**, 2187.
- N. Ö. Can, D. Osmaniye, S. Levent, B. N. Sağlık, B. Inci, S. İlgin, Y. Özkay and Z. A. Kaplancıklı, *Molecules*, 2017, **22**, 1381.
- F. Tok, Z. Uğraş, B. N. Sağlık, Y. Özkay, Z. A. Kaplancıklı and B. Koçyiğit-Kaymakçıoğlu, *Bioorg. Chem.*, 2021, **112**, 104917.



34 F. Tok, B. N. Sağlık, Y. Özkar, S. İlgn, Z. A. Kaplancıklı and B. Koçyiğit-Kaymakçıoğlu, *Bioorg. Chem.*, 2021, 105038.

35 J. Cheung, M. J. Rudolph, F. Burshteyn, M. S. Cassidy, E. N. Gary, J. Love, M. C. Franklin and J. J. Height, *J. Med. Chem.*, 2012, **55**, 10282–10286.

36 C. Binda, J. Wang, L. Pisani, C. Caccia, A. Carotti, P. Salvati, D. E. Edmondson and A. Mattevi, *J. Med. Chem.*, 2007, **50**, 5848–5852.

37 *L. Schrödinger*, Schrödinger, LLC, New York, NY, USA, 2020.

38 M. Alipour, M. Khoobi, A. Foroumadi, H. Nadri, A. Moradi, A. Sakhteman, M. Ghandi and A. Shafiee, *Bioorg. Med. Chem.*, 2012, **20**, 7214–7222.

39 Z. F. Al-Rashid and R. P. Hsung, *Bioorg. Med. Chem. Lett.*, 2015, **25**, 4848–4853.

40 D. Genest, C. Rochais, C. Lecoutey, J. Sopkova-de Oliveira Santos, C. Ballandonne, S. Butt-Gueulle, R. Legay, M. Since and P. Dallemagne, *MedChemComm*, 2013, **4**, 925–931.

41 Y. Zong, J. Wang, P. An, G. Yue, Y. Pan and X. Wang, *Appl. Organomet. Chem.*, 2017, **31**, e3762.

42 L. Yurttaş, Z. A. Kaplancıklı and Y. Özkar, *J. Enzyme Inhib. Med. Chem.*, 2012, **28**, 1040–1047.

43 S.-Y. Son, J. Ma, Y. Kondou, M. Yoshimura, E. Yamashita and T. Tsukihara, *Proc. Natl. Acad. Sci. U. S. A.*, 2008, **105**, 5739–5744.

44 *Maestro*, Schrödinger, LLC, New York, NY, USA, 2020.

45 *LigPrep*, Schrödinger, LLC, New York, NY, USA, 2020.

